

J. Electroanal. Chem., 306 (1991) 111–124
Elsevier Sequoia S.A., Lausanne

The effects of mercury film electrode morphology on square wave voltammetric peak current response as a function of frequency

Samuel P. Kounaves and Wen Deng

Department of Chemistry, Tufts University, Medford, MA 02155 (USA)

(Received 1 August 1990; in revised form 6 November 1990)

Abstract

The net peak-current response as a function of frequency, for both direct and stripping square-wave voltammetry at mercury film electrodes, can differ significantly from theory when either the surface morphology of the mercury film deviates from being a true flat film or the substrate interacts with the analyte in some manner. Mercury layers of various morphologies (film, patches or droplets) and thicknesses (1.0 to 24.0 μm) were prepared by depositing Hg(II) onto an iridium or glassy carbon substrate. Test solutions of Cd(II), Pb(II) and $\text{K}_4\text{Fe}(\text{CN})_6$ in 0.1 M potassium nitrate were used. For square-wave frequencies of 10 to 2000 Hz, the iridium electrodes with true mercury films and the bare Ir electrodes gave a theoretical response for both direct SWV and SWASV with all analytes tested. For the Hg films on glassy carbon or the non-solid Hg-film on Ir, the peak-current response for direct SWV began to decrease at SW frequencies of 900 and 100 Hz respectively. The effect with SWASV was more pronounced, the decrease occurring at 100 and 50 Hz. This behavior is attributed to several factors but mainly to the increased exposure of the substrate as a result of the decreasing thickness of the diffusion layer, and the behavior of the mercury droplets as a collection of ultramicroelectrodes.

INTRODUCTION

In conjunction with various classical voltammetric methods, the mercury film electrode (MFE) has been used successfully and routinely for many years in analytical determinations of metal ions in solution [1]. The most widely used MFE consists of a glassy-carbon substrate coated with a submicron layer of mercury droplets (GCMFE). The use of the MFE with square wave voltammetry (SWV) has become more frequent in the past few years and promises to give advantages of increased sensitivity and good discrimination against background currents [2,3]. The theory, both for square wave direct voltammetry (SWDV) and square wave anodic stripping voltammetry (SWASV) of mercury soluble metals at the MFE, has been given in several publications [4–6]. Calculations based on this theory predict that for

a thin mercury film the net (or differential) peak current Δi_p (the net current Δi at any point is equal to the difference between the forward and reverse currents, $i_f - i_r$) will be proportional to the SW frequency (f) raised to the one-half power for SWDV and to the first power for SWASV. In general, experimental results for SWV and SWASV have been shown to be in excellent agreement with theory [7–9]. However, there have been anomalies noted in several of the studies, especially when mercury film electrodes are used. For both SWDV and SWASV the experimental net peak current Δi_p or peak stripping current Δi_{sp} , respectively, begins to decrease substantially below theoretically predicted values at higher SW frequencies.

In the early work with SWV, Turner et al. [10] referred to unspecified problems with charging currents caused by high SWV frequencies. Later studies by Wechter et al. [3] utilizing a wall-jet GCMFE for SWASV of a 0.5 μM Pb(II) solution, found that the peak stripping current (Δi_{sp}) as a function of SW frequency deviated from theory at values > 50 Hz. They attributed this behavior to the possibility that at higher frequencies the usual model for voltammetry at Hg films may not apply to SWV. Kumar and Heineman [11] combined SWV and SWASV with a thin-layer electrochemical cell. They performed SWV on 200 μM $\text{K}_4\text{Fe}(\text{CN})_6$ solutions and noted a near linear relationship between Δi_p and $f^{1/2}$ in the range of 5 to 500 Hz. However, for $f > 1000$ Hz, the increase in Δi_p was nonlinear. They attributed this behavior to charging currents as previously reported [10]. In an in-depth study of SWV at MFEs, Schreiner [12,13] demonstrated that not only does this anomaly occur with metal analytes in aqueous solution, but also with nitrobenzene in acetonitrile. She suggested that in general the non-theoretical behavior could be attributed to the geometry of the mercury layer and in many cases to adsorbed organic species on the exposed carbon surface interfering with the anticipated behavior of a pure mercury surface. She also noted that the most apparent cause of the decrease of Δi_p with increasing f was the decrease and eventual disappearance of the reverse current component (i_r) of Δi_p . In a preliminary attempt to elucidate this problem, Kounaves and Osteryoung [7] used 5 mm and 127 μm iridium-based MFEs on which the morphology of the mercury was varied from true film to droplets. They found that the maximum attainable SW frequency increased as the film was varied from droplets through patches to true film. However, the large size difference of their electrodes may have complicated matters, in that the 5 mm electrode was too large to support a well formed Hg film and the 127 μm may have behaved as a microelectrode at higher frequencies. To confound the question even further, in the study by Wechter and Osteryoung [9] utilizing a 127 μm iridium based MFE, they observed similar behavior as reported previously, but unlike the GCMFE [12] or the droplet covered IrMFE [7], the mercury film on their iridium substrate was a continuous cohesive layer. Surprisingly, it was also the reverse current component (i_r) of Δi_p that deviated. It was difficult to explain these observations, since i_r in each case corresponds to different processes. Finally, Wikiel and Osteryoung [8], in confirming the theory experimentally for SWV and SWASV using 0.5 mm and 25 μm silver based MFEs (SBMFE), found excellent agreement with theory over a wide range of mercury film thicknesses (0.25–8 μm)

and frequencies (6–600 Hz), except for the smaller electrode where they found a decrease in the reverse current consistent with the results of Wechter and Osteryoung [9]. They suggested that these anomalies may have something to do with electrode size.

This paper describes the results of work undertaken to elucidate this apparent discrepancy and expands on the preliminary results obtained previously [7]. In this study we used both glassy carbon and iridium of similar size as the substrates for the deposition of the mercury film. Iridium has been shown to be insoluble in mercury and, by proper selection of electrolyte and potential, the morphology of the mercury layer can be controlled to give droplets, patches, or true films [14]. For comparative purposes we also used the same electrodes without any mercury film and with $K_4Fe(CN)_6$ as the analyte.

EXPERIMENTAL

Apparatus

Deposition of mercury films and square wave voltammetry experiments were carried out using an EG&G PARC Model 273 potentiostat/galvanostat (EG&G PAR, Princeton, NJ) controlled by an IBM PS/2-30286 computer. Custom software provided all generation of square wave forms and display of resulting data. Unless otherwise indicated, the square wave step height was 5 mV and the pulse amplitude (half peak-to-peak) was 25 mV.

Two types of working electrodes were used; a custom made 2.0 mm diameter iridium disk embedded in a glass capillary with the tip ground flat; and two identical glassy carbon electrodes with a 3.0 mm radius disk embedded in glass (Koslow Scientific, Edgewater, NJ). The electrodes were polished using a high speed rotating wheel with 600 grit and 1200 grit silicon carbide (CARBIMET[®], Buehler Ltd.), and successively hand-polished with 1.0, 0.3, and 0.05 μm alumina (MICRO-POLISH[®], Buehler Ltd.). The electrochemical pretreatment of the iridium surface and deposition of the mercury film were carried out as previously described [14]. The morphology of the film was observed in-situ using a Metaval-H (Leco/Jena) inverted polarizing microscope with a special electrochemical cell and a 35 mm Pentax camera for micro-photography. The reference electrode, to which all potentials are referred, was a saturated sodium chloride calomel reference (SSCE) separated from the test solution by a 0.1 M NaNO_3 salt bridge. A platinum wire was employed as the auxiliary electrode.

Reagents

The lead(II) and cadmium(II) solutions were prepared from their respective nitrate salts (Aldrich Chemical, Milwaukee, WI), the mercury plating solutions from mercury(II) chlorate (Mallinckrodt), and the supporting electrolytes from analytical-grade potassium nitrate (Aldrich) or perchloric acid (Baker Ultrex). All solutions were prepared with 18 $M\Omega$ cm water from a Barnstead Nanopure deionization/filtration system. Solutions were purged with nitrogen for about 30

min before each experiment, with a nitrogen blanket being maintained at all other times. All experiments were run in solutions without stirring. Unless otherwise indicated all test solutions contained 0.1 M KNO_3 and 1×10^{-4} M Cd^{2+} .

Mercury-film morphology

In order to facilitate the description of the mercury layer, the physical form of the mercury on the surface has been categorized into four types of coverage as shown in Fig. 1a–d; (a) a true film covering 99.9% of the surface, save for a few films where a partial “hairline” exposure of the edge sometimes occurred, (b) large patches, with only small thin sections of exposed surface, covering about 90% of the surface, (c) small patches covering 50–60% of the surface, and (d) a homogeneous layer of mercury droplets covering approximately 50% of the surface. The droplet and patchy films were formed on the 2 mm iridium and 3 mm glassy carbon electrodes, while the true films were formed only on the 2 mm iridium electrode. The thickness of the films reported below is the thickness which would be expected for the deposition of an ideal flat mercury film. This means that, except for the thin flat films, the thickness at the center of a thick true film or of a droplet layer film may be, respectively, 2 to 6 times greater than assumed [15]. All electrodes were observed in-situ continuously to insure that the morphology of the mercury layer did not undergo any changes during an experiment.

RESULTS

Square wave direct voltammetry

The theory for SWDV at mercury film electrodes [4] predicts the shape and position of the SW voltammogram as a function of the thickness and frequency

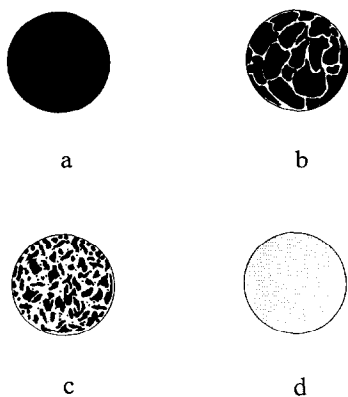


Fig. 1. The morphology of mercury on the surface categorized into four types of coverage; (a) a true film covering 99.9% of the surface, (b) large patches, with only small thin sections of exposed surface, covering about 90% of the surface, (c) small patches covering 50–60% of the surface, and (d) a homogeneous layer of mercury droplets covering approximately 50% of the surface.

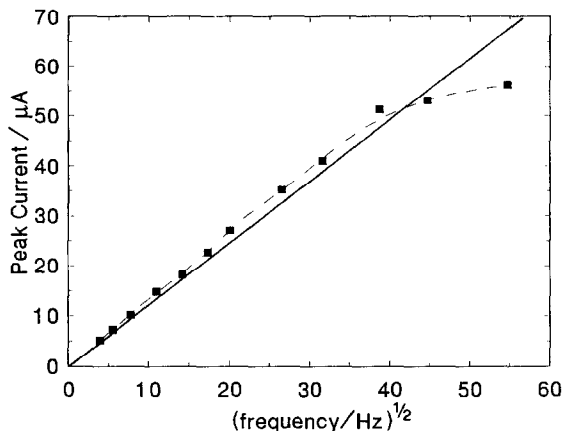


Fig. 2. Experimental (■ — — ■) and theoretical (—) SWDV data for a true mercury film on 2.0 mm iridium substrate, with $l = 18 \mu\text{m}$, and $1.6 \times 10^{-6} \text{ M Pb(II)}$ in 0.1 M HClO_4 (other conditions given in text).

according to the dimensionless parameter Λ , defined as

$$\Lambda = l(f/D_R)^{1/2} \quad (1)$$

where l is the film thickness, f is the SW frequency, and D_R is the diffusion coefficient of the metal in mercury. For very thin films or very low frequencies ($\Lambda < 0.3$), the net peak current $\Delta i_p = \text{Cottrell current} \times 1.500$. For thick films or very high frequencies ($\Lambda > 3$), we have $\Delta i_p = \text{Cottrell current} \times 1.312$. For $0.3 < \Lambda < 3$, the value of the constant changes from 1.312 to a maximum of 1.981 and back to 1.500. For any given film thickness then, we should see a constant increase in net peak current with increasing SW frequency except for a slightly accelerated increase (hump) around the point where the diffusion length is equal to the film thickness, i.e. when $l \approx (D_R/f)^{1/2}$.

An example of experimental and theoretical data for a true mercury film with $l = 18 \mu\text{m}$ on the 2.0 mm iridium substrate, using $1.6 \times 10^{-6} \text{ M Pb(II)}$ in 0.1 M HClO_4 is shown in Fig. 2. The experimental net peak current, Δi_p , is in agreement with theory up to a frequency of $\approx 1600 \text{ Hz}$. Similar results have been obtained by us using Cd(II) and also by others in studies with true mercury films on silver [8] and with the hanging mercury drop electrode. Thus, we know that at high SW frequencies both the $\text{Cd}^{2+}/\text{Cd}^0$ and $\text{Pb}^{2+}/\text{Pb}^0$ systems behave reversibly in the above solutions at a mercury surface with excellent correlation to theory. There were several conditions during this set of experiments under which we obtained non-theoretical performance with these electrodes. As can be seen in Fig. 2 for $f > 1600 \text{ Hz}$ there is a slight decrease in Δi_p . We are reasonably certain that this deviation is due to limitations in the electronics of the instrument and cell. Observation of the waveform with an oscilloscope shows a tendency for the square waveform to become slightly skewed with rounded edges at $f > \text{ca. } 1500 \text{ Hz}$. This same problem

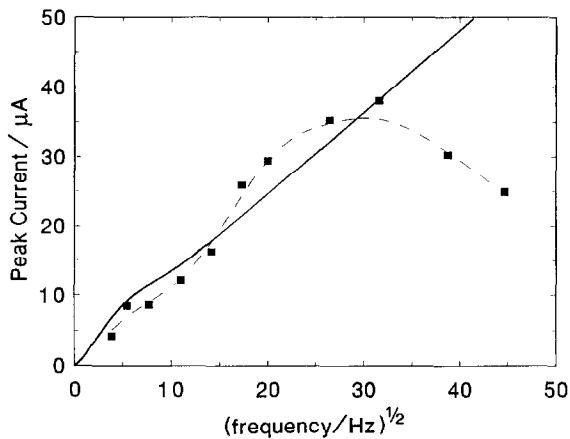


Fig. 3. Experimental (■ — — ■) and theoretical (—) SWDV data for a mercury film on 2.0 mm iridium substrate, with $l_{\text{app}} = 8.5 \mu\text{m}$, and $1 \times 10^{-4} \text{ M Cd(II)}$ in 0.1 M KNO_3 (other conditions given in text).

and suggested cause have been reported in several previous investigations [10,11]. A more severe deviation was noticed several times, usually with a 30% decrease of Δi_p and/or appearance of a second peak for $f > 500 \text{ Hz}$. However, upon careful observation it was clear that the edge of the iridium substrate was exposed. It may be one of the reasons that similar deviations were observed in previous experiments using true mercury films on large silver and iridium substrates [8,9].

Figure 3 shows the data for the iridium substrate on which a patchy film (Fig. 1b) was deposited, with the total charge used being equivalent to that for deposition of a $8.5 \mu\text{m}$ thick flat film (l_{app}). The experimental data agrees reasonably well with mercury film theory for values of $f > 900 \text{ Hz}$, above which the net current peak becomes wider and decreases. If less mercury is deposited so that the patches are even smaller and more of the substrate is exposed (Fig. 1c), the results shown in Fig. 4 are obtained. The data here are for the iridium substrate and a mercury film equivalent to a $6.2 \mu\text{m}$ flat film. What is immediately noticeable with this film, and not seen with any of the other types of films, is the sudden appearance of a second peak (-0.70 V vs. SSCE) starting at $f \approx 25 \text{ Hz}$. At the same time the primary peak (-0.65 V vs. SSCE) reaches a maximum value at $f \approx 300 \text{ Hz}$ and then begins to decrease. This phenomenon was observable on four of six electrodes made with similar mercury film thickness and morphology. This same behavior has also been observed on a 5 mm iridium electrode in the previous study [7].

If mercury is deposited for a shorter time, the mercury patches become smaller, and eventually only droplets cover the surface. Figure 5 shows an example of experimental and theoretical data for a droplet film on the iridium substrate with $l_{\text{app}} = 3.6 \mu\text{m}$. The experimental net peak current is basically in agreement with theory up to a frequency of approx. 60 Hz; it then begins declining, until it levels off around 200 Hz. This type of behavior is exhibited by all the iridium mercury droplet

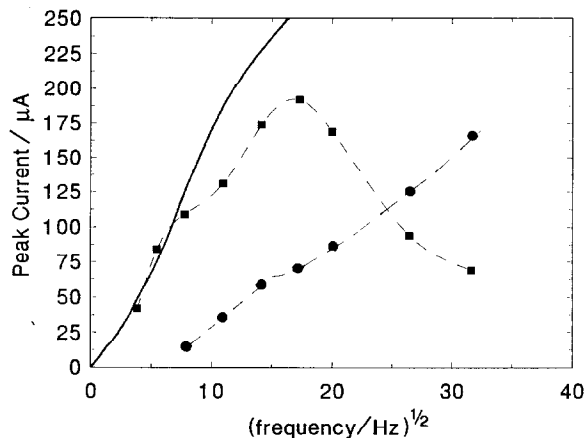


Fig. 4. SWDV experimental data for the apparent red/ox of Cd from Hg (■— — ■) and from Ir (●— — ●). (—) Theoretical data for a mercury film on a 2.0 mm iridium substrate, with $l_{app} = 6.2 \mu\text{m}$, and $1 \times 10^{-4} \text{ M Cd(II)}$ in 0.1 M KNO_3 (other conditions given in text).

film electrodes made, although the exact frequency where the maximum Δi_p value occurs varies between 50 to 100 Hz. This is the same behavior as noted for mercury droplet films formed on glassy carbon as described below and also by Wechter et al. [3] and Schreiner [12,13], but in those cases the Δi_p maximum occurs at approx. 250 Hz.

The data for the GCMFEs was very similar to previous studies [3,7,12,13]. As will be discussed further below, all mercury films regardless of thickness showed the

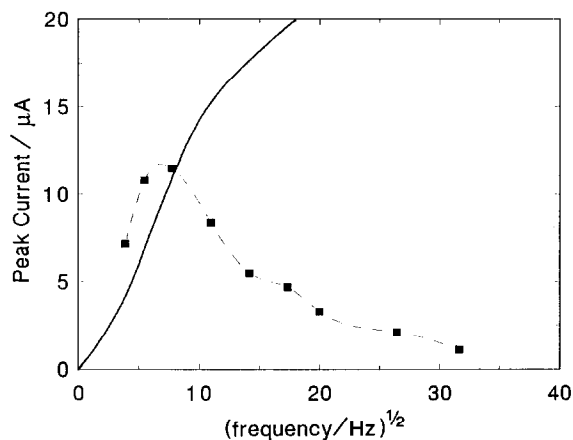


Fig. 5. Experimental (■— — ■) and theoretical (—) SWDV data for a mercury film on 2.0 mm iridium substrate, with $l_{app} = 8.5 \mu\text{m}$, and $1 \times 10^{-4} \text{ M Cd(II)}$ in 0.1 M KNO_3 (other conditions given in text).

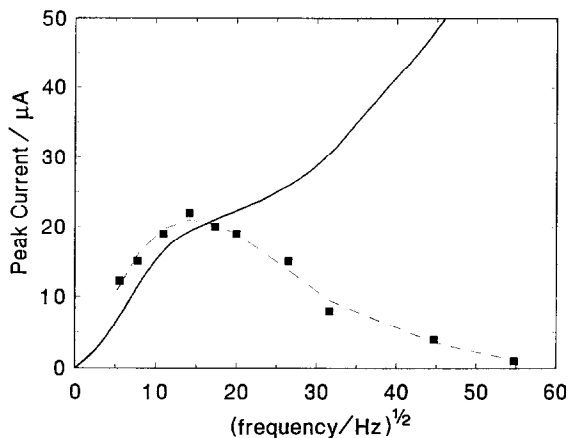


Fig. 6. Experimental (■ — — ■) and theoretical (—) SWDV data for a mercury film on a 3.0 mm glassy carbon substrate, with $l_{\text{app}} = 2.7 \mu\text{m}$, and $1 \times 10^{-4} \text{ M Cd(II)}$ in 0.1 M KNO_3 (other conditions given in text).

same deviation from SWV theory at frequencies varying from 200 to 500 Hz. Figure 6 shows a typical response for the 3 mm GCMFE with $l_{\text{app}} = 2.7 \mu\text{m}$.

Finally, using the GCMFE and the IrMFE without a mercury film in a 0.1 M KNO_3 , $6 \text{ mM K}_4\text{Fe(CN)}_6$ solution, we found that Δi_p for the bare GC substrate decreased substantially for $f > 50 \text{ Hz}$, implying the existence of an interaction between analyte and surface. For the bare Ir substrate Δi_p decreased only slightly for $f > 800 \text{ Hz}$.

Square wave anodic stripping voltammetry

As with SWDV, the theory for SWASV [5] predicts that for values of $\Lambda > 3$ the net stripping peak current, Δi_{sp} , will equal the Cottrell current $\times 1.312$. However, in contrast to SWDV, for $3 > \Lambda > 0.3$ there is a sudden decrease to approx. 0.1 of the Cottrell current, after which, for $\Lambda < 0.3$, $\Delta i_{\text{sp}} = 0.298nQ_R f$ (where Q_R = deposition charge and n = number of electrons). Figure 7 shows a representative result for a true mercury film on the iridium substrate with $l = 2.1 \mu\text{m}$, and a deposition time of 5 s. The net peak stripping current is almost 50% lower than predicted but follows the overall shape of the theoretical curve. This lower value, however, is not unexpected, since the use of the experimentally measured deposition time and current to calculate Q_R and/or c_R^* can introduce a significant error.

Using a mercury film composed of small patches (Fig. 1c), we obtained results as shown in Fig. 8. In this sample the MFE consisted of the iridium substrate with an equivalent $3.3 \mu\text{m}$ thick mercury film, with a Cd(II) deposition time of 5 s. In contrast to the SWDV results (for the same type of film), the change of net peak stripping current, Δi_{sp} , with frequency does not exhibit a maximum and then decline, but undergoes a change in slope between 100 and 200 Hz and continues to

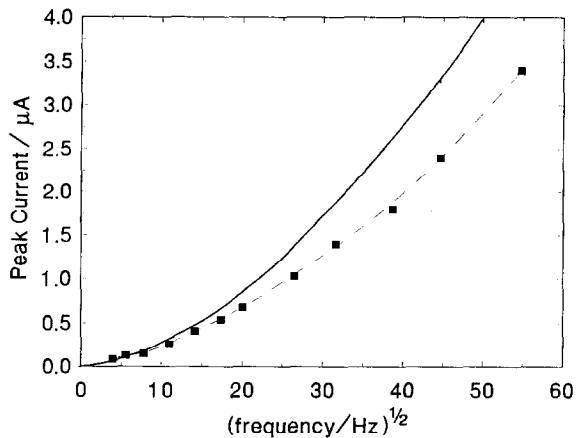


Fig. 7. Representative result of SWASV experimental (■— — ■) and theoretical (—) data for a true mercury film on a 2.0 mm iridium substrate, with $l = 2.1 \mu\text{m}$, 5 s deposition time, and $1 \times 10^{-4} \text{ M}$ Cd(II) in 0.1 M KNO_3 (other conditions given in text).

increase. These results are similar to those obtained by Wechter et al. [3] for Pb^{2+} at a glassy carbon MFE.

Mercury films composed of droplets on Ir or GC gave results very similar to those reported by Wechter et al. [3] and Kounaves and Osteryoung [7]. Overall, the behavior of SWASV with patchy or droplet mercury films at SW frequencies > 100 Hz was not very consistent. Repeated attempts with Pb^{2+} , Cd^{2+} , and different electrodes, gave no improvement in signal or reproducibility. In many cases the

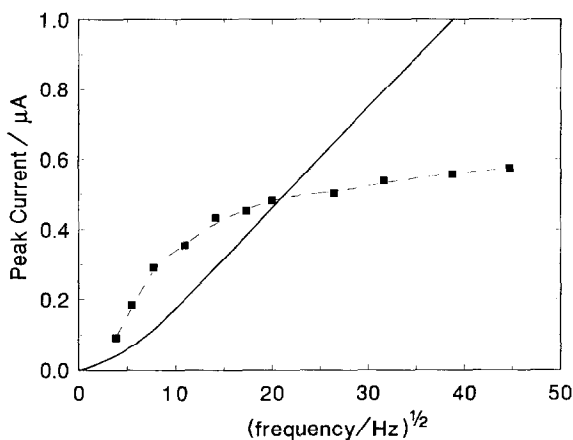


Fig. 8. Representative result of SWASV experimental (■— — ■) and theoretical (—) data for a mercury film on a 2.0 mm iridium substrate, with $l_{\text{app}} = 3.3 \mu\text{m}$, 5 s deposition time, and $1 \times 10^{-4} \text{ M}$ Cd(II) in 0.1 M KNO_3 (other conditions given in text).

morphology of the droplet film appeared to undergo significant changes during the deposition-stripping cycle.

DISCUSSION

From all our data above and previous works it appears reasonable that for both SWDV and SWASV more than one mechanism is responsible for the reported decreases of Δi_p and Δi_{sp} , respectively. We have separated the mechanisms responsible into four broad categories related to: (i) diffusion layer response to high frequencies in SWV, (ii) surface reaction kinetics, (iii) microelectrode behavior, and (iv) instrumental limitations. We will limit the major portion of the discussion here to topic (i), since we believe this is what brings about the problems with mechanisms (ii) and (iii), and which will be dealt with in more detail in a later paper.

Frequency effects on the diffusion layer thickness

The morphology of the mercury film and its interaction with the diffusion layer and the surface current distribution presents a very difficult problem since many complicating factors enter the picture.

For SWDV on the iridium MFE, it appears evident from the data in Figs. 2 to 5 that the progressive decrease in current is related initially to the increasingly exposed iridium surface. This becomes very clear in Fig. 4, where the appearance of a very prominent second peak (occurring about 150 mV more negative than the primary peak) is due to the red/ox of the cadmium on the exposed iridium surface. However, that this second peak diminishes and disappears with the mercury droplet electrodes, implies that when the mercury droplets are deposited in smaller size and greater numbers, the cadmium red/ox again takes place at the mercury, but Δi_p continues to be reduced by some other factor. Whatever this factor may be, it appears to operate on both the Ir and GC based droplet MFEs under most conditions.

In the case of SWDV on the GCMFE, the observations are very surprising. We have compiled in Fig. 9 all the data from this study and two points from the published work of Schreiner [12]. The plot shows the maximum SW frequency attainable at these GCMFEs before a non-theoretical response appears, as a function of the thickness of the mercury film deposited. In this case, since the "films" on the GCMFEs are always in the form of droplets, the thickness is always, in effect, an indirect indicator of the droplet size and of the percent surface coverage. As can be seen in Fig. 9, there is a film thickness (i.e., droplet density/size) at which a maximum frequency response is attained. This "film" thickness, as we shall see below, corresponds to a droplet size of the same order as the diffusion layer thickness.

It is extremely difficult to make any sort of quantitative comparison between the data for the two types of electrodes. Even though some of the mercury films are the same apparent thickness, we must remember that the mercury on the GC is in the form of spheres while on the iridium it is in the form of semispheres (i.e., partial

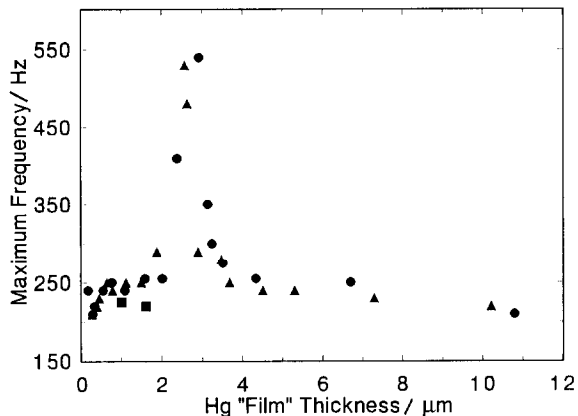


Fig. 9. Maximum SW frequency attainable at GCMFEs from this work (●, ▲) and ref. 12 (■) before non-theoretical response appears, as a function of the thickness of the mercury film deposited. Since the "films" on the GCMFEs are always in the form of droplets, the thickness is an indirect indicator of the droplet size and of the percent surface coverage (other conditions given in text).

segments of a sphere), thus the two morphologies do not display the same fraction of coverage at the same thickness. In addition, the Hg drops are free to move about on the GC but not on the Ir surface, so that the coalescence process occurs differently on the two. Taking all of this into account, it is still possible to make some qualitative comparisons between the two types of electrodes. For very thin film electrodes the peak frequency is in the 50 to 200 Hz range and both IrMFEs and GCMFEs display the same morphology and current-frequency response. As the films are made more dense, the GCMFEs reach their maximum peak frequency at about 500 to 600 Hz (Fig. 9) while at the same point the IrMFEs are still on an approximately linear increase and are at about 800 to 1000 Hz. At this point their similarities end. The peak frequency response of the GCMFEs falls back to the 200 to 250 Hz range as the droplets coalesce on the surface to form larger spheres. At the IrMFEs we have reached a point where a true mercury film can form on their surfaces, and the maximum peak frequency is limited by electronics.

The two scenarios for the GC and IrMFEs are very similar except for the inherent differences in the surface morphologies of the mercury. In our opinion, the phenomenon occurring at both results directly from the dependence of the diffusion layer thickness on the SW frequency. The influence of the surface morphology (microprofile) on electrochemical deposition processes is well documented [16,17]. As the diffusion layer becomes thinner with increasing SW frequency, the surface morphology becomes more important. The thickness of the Nernst diffusion layer for a square wave potential is given by [16]:

$$\delta_N = 2.92(D_O/f)^{1/2} \quad (2)$$

where f is the SW frequency, and D_O is the diffusion coefficient of the ion in solution. In deriving eqn. (2), Despic and Popov [16] have shown that δ_N after the

TABLE 1

Diffusion layer thickness (δ_N) as a function of SW frequency (f) for Pb^{2+} ($D_O = 6.97 \times 10^{-6} \text{ cm}^2/\text{s}$)

Frequency/Hz	Diffusion layer thickness/ μm
10	25
50	11
100	7.8
200	5.5
500	3.4
1000	2.5
2000	1.7

n th pulse is not significantly different from that at the end of the first pulse. Thus the latter can be taken as an indication of the diffusion situation for a square waveform potential. In effect, δ_N for a square waveform does not expand but stays constant, determined only by the SW frequency. Table 1 lists some values of δ_N as a function of f for $\text{Pb}(\text{II})$ ($D_O = 6.97 \times 10^{-6} \text{ cm}^2/\text{s}$). If we look at the calculated values of δ_N and compare them with the drop size existing at a given film thickness, we find that δ_N is of the same size as the drop diameter. Figure 10 shows diagrammatically the qualitative observations of the GC surfaces at various Hg film thicknesses and SW frequencies. What appears to be happening is that at low values of f and with a small number of Hg droplets on the surface, δ_N is large enough so that we have linear diffusion to the droplets with very little to the substrate surface. As f increases, both diffusion to the surface and spherical diffusion become predominant and start to limit the current. With the greater surface coverage by droplets, it takes a much higher frequency to reach the same conditions, until we have an ideal "match" between δ_N and drop size/density. At that point we attain

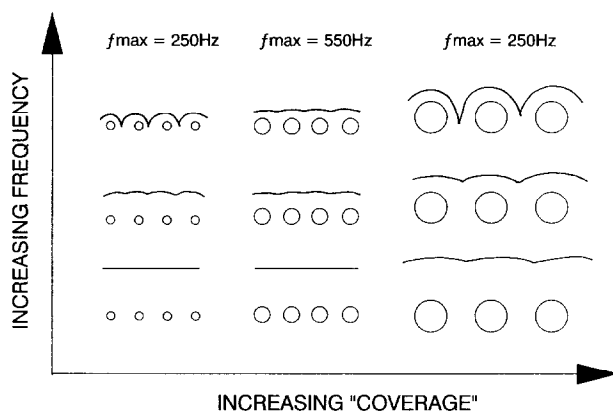


Fig. 10. Diagrammatic representation of the qualitative observations of the Hg "film" morphology on glassy carbon at increasing Hg film thickness and SW frequency.

the f_{\max} seen in Fig. 9. If the Hg droplets become too large, both the space between them and spherical diffusion take over earlier and non-theoretical behavior begins at a lower f .

In summary, what we have is the thickness of the diffusion layer “setting up” the proper conditions so that other limiting factors such as, spherical diffusion and/or surface reactions and kinetics can become dominant.

Surface reaction kinetics

Once the value of δ_N has become small enough to allow direct reaction of the surface with the analyte, the systems become more intractable to characterize. In the case of the GC electrode even the well known redox reactions of ferri/ferro-cyanide are not known to behave properly, especially with SWV [18]. For this system we must presume that the reaction mechanism is a first-order slow electron transfer and as such we would expect Δi_p to decrease, along with an increase in peak width and negative shift in peak potential [19]. In addition this behavior would become predominant for small enough rate constants or for higher frequencies. This is exactly what appears to occur with both the GCMFE and the bare GC.

Microelectrode behavior

With smaller δ_N values, one can easily conceive of a point (barring any surface reaction effects) at which the Hg droplet film would begin to behave as an assembly of Hg microelectrodes. The current theories describing SWV for linear diffusion at mercury electrodes [4,5] are valid when $r(f/D_O)^{1/2} \gg 1$. For example, at the Hg droplets on the GC or Ir surface with Pb(II) as the ion, and spherical drops of about 5 μm diameter, SWV requires a $f \leq 100$ Hz. Even though the behavior of SWV at microelectrodes has been developed [20], no such theory for SWV at Hg microelectrodes with metal ions has been developed. Work is currently underway towards elucidating this problem.

Instrumental limitations

There are certain electronic limitations inherent in trying to drive potentiostatic circuits and electrochemical cells, designed for static or low frequencies, at the higher frequencies required with SWV. These limitations are probably responsible for the non-theoretical behavior at both bare glassy carbon electrodes and IrMFEs for $f > 1000$ Hz [10,11] and where no other surface reactions occur. In general this limitation is of minor importance and can be overcome by designing high frequency compatible SWV instrumentation and cells.

CONCLUSION

The data obtained from this and previous studies, indicate a complex set of mechanisms occurring at the surface of mercury film electrodes under the conditions of SWV. Even though all of the problems and observations have not been fully addressed here, especially in terms of the reverse current behavior in both SWV and

SWASV, we feel that there is enough evidence to point to the decreasing thickness of the diffusion layer as the prime source of the non-theoretical behavior of SWV at high frequencies at these MFEs. Square Wave Voltammetry is a sensitive and powerful electroanalytical technique and further studies are warranted in order to separate and identify the individual causes of this anomalous behavior at MFEs.

ACKNOWLEDGEMENTS

The authors gratefully acknowledge the helpful discussions with Janet Osteryoung and Mary M. Schreiner at SUNY-Buffalo, where the preliminary work reported in ref. 7 was carried out.

REFERENCES

- 1 T.F. Florence, *J. Electroanal. Chem.*, 27 (1970) 273.
- 2 J.G. Osteryoung and R.A. Osteryoung, *Anal. Chem.*, 57 (1985) 101A.
- 3 C. Wechter, N. Sleszynski, J.J. O'Dea and J. Osteryoung, *Anal. Chim. Acta*, 175 (1985) 45.
- 4 S.P. Kounaves, J.J. O'Dea, P. Chandrasekhar and J. Osteryoung, *Anal. Chem.*, 58 (1986) 3199.
- 5 S.P. Kounaves, J.J. O'Dea, P. Chandrasekhar and J. Osteryoung, *Anal. Chem.*, 59 (1987) 386.
- 6 M. Penczek and Z. Stojek, *J. Electroanal. Chem.*, 213 (1986) 177.
- 7 S.P. Kounaves and J. Osteryoung, Pittsburgh Conference, Atlantic City, NJ, March 1987, Abstr. 179.
- 8 K. Wikiel and J. Osteryoung, *Anal. Chem.*, 61 (1989) 2086.
- 9 C. Wechter and J. Osteryoung, *Anal. Chem.*, 61 (1989) 2092.
- 10 J.A. Turner, U. Eisner and R.A. Osteryoung, *Anal. Chim. Acta*, 90 (1977) 25.
- 11 V. Kumar and W.R. Heineman, *Anal. Chem.*, 59 (1987) 842.
- 12 M.M. Schreiner, Ph.D. Thesis, SUNY Buffalo, New York, 1987, UMI No. 8727741.
- 13 M.M. Schreiner and J. Osteryoung, ref. 7, Abstr. 178.
- 14 S.P. Kounaves and J. Buffle, *J. Electroanal. Chem.*, 216 (1987) 53.
- 15 S.P. Kounaves and J. Buffle, *J. Electroanal. Chem.*, 239 (1988) 113.
- 16 A.R. Despic and K.I. Popov, *J. Appl. Electrochem.*, 1 (1971) 275.
- 17 I. Markov, A. Boynov and S. Toshev, *Electrochim. Acta*, 18 (1973) 377.
- 18 K.H. Wong and R.A. Osteryoung, *Electrochim. Acta*, 32 (1987) 629.
- 19 J.J. O'Dea, J. Osteryoung and R.A. Osteryoung, *Anal. Chem.*, 53 (1981) 695.
- 20 D.P. Whelan, J.J. O'Dea, J. Osteryoung and K. Aoki, *J. Electroanal. Chem.*, 202 (1986) 23.